

Clinical and chest computed tomography characteristics from 58 Patients with COVID-19 pneumonia and correlations with disease length and severity

W. Li^{1,2*} and Y. Zhou^{1,2}

¹Department of Pulmonary and Critical Care Medicine, the Third Affiliated Hospital of Sun Yat-sen University, Guangzhou, China

²Hubei Medical Team of the Third Affiliated Hospital of Sun Yat-sen University, Guangzhou, China

ABSTRACT

► Original article

*Corresponding author:

Wenjuan Li, Ph.D.,

E-mail:

liwenjuan@mail.sysu.edu.cn

Received: March 2022

Final revised: September 2022

Accepted: January 2023

Int. J. Radiat. Res., April 2023;
21(2): 281-291

DOI: 10.52547/ijrr.21.2.15

Keywords: SARS-CoV-2, chest CT, Covid-19, disease severity, outcomes.

Background: This study aimed to review computed tomography (CT) findings in COVID-19 patients, and establish correlations between CT findings in patients with a short vs. long disease course, and in those with mild vs. severe disease. **Materials and Methods:** From February 2020 to March 2020, 58 patients with SARS-CoV-2 infections were retrospectively included. Clinical, laboratory, and CT findings were compared between patients with a short vs. long disease course, and in subgroups with mild vs. severe disease. Correlation analyses were performed to determine factors correlated to greater disease severity in patients with short/long disease courses, respectively. **Results:** Fifty-eight patients were included; 29 in the short disease course and 29 in the long disease course group. CT findings were similar between patients with a short and a long disease course (all, $P > 0.05$). Among the short disease course group, severe disease patients had significantly higher rates of right upper lobe involvement, 5 lobes affected, pericardial effusion, pleural involvement and bilateral pleural thickening, grid shadow, higher-density vascular shadows, crazy-paving appearance, lung consolidation, an air bronchogram sign, and fibrous foci than those with mild disease. Among the long disease course group, severe disease patients had significantly higher rates of right upper lobe and middle lobe involvement, 5 lobes affected, pleural effusion and thickening, grid shadow, higher-density vascular shadows, crazy-paving appearance, lung consolidation, an air bronchogram sign, and atelectasis. **Conclusions:** CT imaging findings may help to predict disease severity in COVID-19.

INTRODUCTION

Many pneumonia cases were reported in December 2019 ⁽¹⁾. The pathogen and the disease were named SARS-CoV-2 and novel Coronavirus Disease 2019 (COVID-19), respectively ⁽²⁾. The disease resulted in a worldwide pandemic with more and more persons affected and deaths. Although vaccines have been developed, the disease continues to infect people around the globe as programs to vaccinate persons in every country are put into place.

The virus is spread through respiratory droplets and enters the body via the lungs. It does this by attaching to the receptor angiotensin-converting enzyme 2 (ACE2) via a spike protein, and then subsequently invades the host cells ⁽²⁾. As such, initial clinical symptoms are those of a respiratory tract infection, e.g. cough, fever, shortness of breath. The gold standard for diagnosis of infection is RT-PCR. As the virus infects the lungs radiography has become an important means of identifying the possibility of an infection and following the disease course ^(3, 4).

While chest x-ray is useful for determining a

possible infection and placing a patient in quarantine until a definitive diagnosis can be made ⁽⁴⁾, chest computed tomography (CT) has become the primary radiographic method of diagnosis and following the disease course ⁽⁴⁻⁷⁾. A study using RT-PCR as the reference found that the chest CT imaging sensitivity for the diagnosis of COVID-19 pneumonia was 97% ⁽³⁾. Interestingly, the authors also found that 42% of patients had improved follow-up chest CT before the PCR results became negative.

On the other hand, while chest CT is highly sensitive the specificity is low and it is not recommended to replace RT-PCR for diagnosis ⁽⁸⁾. CT findings common to patients with COVID-19 include ground-glass opacities (GGO), involvement of multiple lobes, focal areas of consolidation, and signs of organizing pneumonia ^(6, 9). Atypical chest CT manifestations of COVID-19 include airway changes, and pleural changes, such as thickening, fibrosis, and nodules ⁽⁷⁾. CT manifestations have also been associated with disease progression and prognosis ⁽⁷⁾.

Serial chest CT imaging is used to assess disease severity and course in COVID-19 patients, and

various radiographic COVID-19 severity scoring systems have been developed ⁽¹⁰⁾. Specific CT findings have been associated with different disease stages, severity, and outcomes ⁽¹¹⁻¹³⁾. However, while studies have provided some consistent findings, inconsistencies between different studies have also been noted. Therefore, the correlation between CT findings and disease outcomes remains to be further investigated in COVID-19 patients. Further data on the ability of CT to predict outcomes in COVID-19 patients may assist in targeting patients who may need more intensive treatment and improving outcomes.

The purpose of this study was to review CT findings in COVID-19 patients, and establish correlations between CT findings in patients with a short vs. long disease course, and in those with mild vs. severe disease.

MATERIALS AND METHODS

Patients and data source

The clinical data and chest CT images of patients with laboratory-confirmed SARS-CoV-2 infections treated by the Hubei Medical Team of the Third Affiliated Hospital of Sun Yat-sen University from February 2020 to March 2020 were retrospectively reviewed.

Inclusion criteria for the study were adult patients with complete demographic and clinical data, disease history, chest CT, and laboratory data (complete blood count, biochemical detection of liver and kidney function, D-dimer level, and levels of inflammatory factors). Only patients with a infection confirmed by laboratory RNA nucleic acid testing (RT-PCR) were included. Patients with an unconfirmed infection or incomplete data were excluded. The endpoint of the study was March 30, 2020.

Data extraction and patient grouping

Data collected from the medical records included age and sex, body mass index (BMI), medical history and comorbidities (e.g., cardiovascular disease, renal failure), smoking history, days from onset of symptoms to CT scan, laboratory data, symptoms on admission (e.g., fever, cough), and CT scan finding (e.g., the number of affected lobes, which lobes were affected, lymphadenopathy, and specific signs such as ground-glass opacity).

Patients were classified according to the length of their disease course: short disease course, 9-18 days from the beginning of symptoms; long disease course, 19-40 days from the beginning of symptoms. The endpoint was defined as March 30, 2020. For further analysis, the short or long disease course groups were further subdivided into mild disease and severe disease patients.

Severe disease was defined as the presence of any

of the following: 1) Breath shortness and a respiratory rate ≥ 30 breaths/minute; 2) Oxygen saturation at rest $\leq 93\%$; 3) $\text{PaO}_2/\text{FiO}_2 \leq 300$ mm Hg at atmospheric pressure; 4) Chest imaging showed lesions progression $\geq 50\%$ within 24-48 hours. When none of the aforementioned criteria were present, the infection was defined as mild disease.

Patient outcomes were classified as discharged, transferred to the ICU, with no obvious change, and symptom improvement at the end of the range of the disease course (i.e., 18 days or 40 days). The reason for transfer to the ICU was worsened disease with respiratory failure requiring mechanical ventilation.

CT scan

Chest CT scans were performed using a SOMATOM Force scanner (Siemens Healthineers, Forchheim, Germany). Scanning parameters were as follows: tube voltage=100-120 kV and a slice thickness=5 mm. The CT dose index volume (CTDIvol) ranged from 3.01 to 5.13 mGy, and the dose-length product (DLP) ranged from 109 to 196 mGy. Patients were placed in the supine position and instructed to hold breath, and images were acquired during a single breath-hold to avoid motion artifacts. Scans were performed from the upper thoracic inlet level to the inferior level of the costophrenic angle.

Image analysis

Images analysis was performed using an Image Archiving and Transmission System (Synapse 3D) by 2 radiologists (with 15- and 5-year experience in thoracic radiology, respectively). The CT was evaluated independently by the radiologists blinded to the patients' clinical, laboratory, and histopathological data. After review, the results were compared, and if they differed a final decision was reached by consensus after discussion.

Statistical analyses

Continuous data were expressed as mean \pm standard deviation and were compared with Student's independent t-test or Mann-Whitney U test (when normality was not assumed). Categorical data were reported as numbers and percentage and were compared with chi-square test or Fisher's exact test (when expected value ≤ 5). Pearson's correlation analysis was used to examine relations among variables. Depending on the data properties, the different correlation coefficients would be used respectively, including Pearson's correlation coefficient, Spearman's correlation coefficient, and point-biserial correlation coefficient. Analyses were also performed based on disease course (short: 9 to 18 days, long: 19 to 40 days). All statistical analysis was performed using IBM SPSS version 25 software (IBM Corporation, Somers, New York). A P-value <0.05 was considered statistical significance.

RESULTS

Among the 59 included patients, and there were 29 in the short disease course group and 29 in the long disease course group. Patient demographic and clinical characteristics are summarized in table 1. The two groups had similar demographic and clinical characteristics. However, the short disease course group had a significantly higher level of high-sensitivity C-reactive protein (hsCRP) than the long disease course group (42.29 ± 49.61 vs. 10.57 ± 12.41 mg/L, $P=0.001$).

The comparison of the characteristics of patients with mild vs. severe disease within the short disease course group and the long disease course group are shown in tables 2 and 3, respectively. Among the short disease course group, severe disease patients had a significantly lower lymphocyte count and serum albumin level, and significantly higher D-dimer, hsCRP, and serum glucose levels than mild disease patients (all, $P<0.05$) (other parameters were similar between groups). Among the long disease course group, severe disease patients had significantly lower albumin levels, and significantly higher D-dimer, hsCRP, lactate dehydrogenase (LDH), and alanine aminotransferase (ALT) levels than mild disease patients (all, $P<0.05$) (other parameters were similar between groups).

CT findings were also compared. All CT findings examined were similar between the short and long disease course groups (all, $P>0.05$, data not shown).

A comparison of CT findings in patients with mild vs. severe disease who had a short disease course is reported in table 4. Patients with severe disease had significantly higher rates of right upper lobe

involvement, 5 lobes affected, pericardial effusion, pleural involvement and bilateral pleural thickening, grid shadow, higher-density vascular shadows, crazy-paving appearance, lung consolidation, an air bronchogram sign, and fibrous foci. A comparison of CT findings in patients with mild vs. severe disease and a long disease course is shown in table 5. Patients with severe disease had significantly higher rates of right upper lobe and middle lobe involvement, 5 lobes affected, pleural effusion and thickening, grid shadow, higher-density vascular shadows, crazy-paving appearance, lung consolidation, an air bronchogram sign, and atelectasis. Severe disease patients were also more likely to have symptom improvement (i.e., improvement of initial symptoms).

To determine factors associated with greater disease severity, correlation analyses were performed of all variables with disease severity in the short and long disease course groups. A summary of the results is shown in table 6. There were many similarities in CT findings in the 2 groups. Of note, however, in the short disease course group, pericardial effusion and fibrous foci were correlated with greater disease severity but not in the long disease course group. On the other hand, bilateral lung involvement, mediastinal lymphadenopathy, and atelectasis were associated with greater disease severity in the long disease course group but not in the short disease course group.

Representative CT images of different findings in COVID-19 patients are shown in figure 1. Serial CT images of a 47-year-old male and a 58-year-old female with COVID-19 are shown in figures 2 and 3, respectively.

Table 1. Patient demographic and clinical characteristics.

Parameter	Short disease course (n = 29)	Long disease course (n = 29)	All (N = 58)	P
Age	66.03±14.41	66.07±11.43	66.05±12.89	0.992
BMI, kg/m ²	24.06±3.15	23.56±3.57	23.85±3.29	0.670
Onset to CT, days	13.66±2.68	24.72±6.18	19.19±7.31	<0.001
WBC count, ×10 ⁹	6.01±2.12	7.09±4.46	6.55±3.51	0.243
Lymphocytes	1.16±0.43	1.42±0.72	1.29±0.60	0.102
Platelet count, ×10 ⁹	246.41±97.45	290.45±91.17	268.43±96.13	0.081
Hemoglobin, g/L	126.59±15.85	120.90±17.92	123.74±17.01	0.206
Prothrombin time, s	13.42±0.82	13.96±1.22	13.68±1.06	0.058
D-dimer, mg/L	1.86±2.58	2.18±3.62	2.02±3.11	0.705
hsCRP, mg/L	42.29±49.61	10.57±12.41	26.43±39.25	0.001
ALT, U/L	37.76±38.25	27.07±26.44	32.41±33.03	0.221
AST, U/L	35.21±27.51	24.31±16.79	29.76±23.25	0.074
Albumin, g/L	36.48±4.60	36.18±4.57	36.33±4.55	0.806
Total bilirubin, μmol/L	11.29±6.64	9.29±5.71	10.29±6.22	0.224
LDH, U/L	301.72±151.09	266.41±99.65	284.07±128.10	0.298
Creatinine, μmol/L	79.76±32.11	87.21±105.32	83.48±77.26	0.717
Glucose, mmol/L	6.97±2.97	6.72±2.89	6.84±2.91	0.746
Procalcitonin, ng/ml	0.14±0.16	11.94±62.73	6.26±45.16	0.342
Sex				0.599
Male	15 (51.72)	13 (44.83)	28 (48.28)	
Female	14 (48.28)	16 (55.17)	30 (51.72)	
Age, years				0.785
< 65	10 (34.48)	11 (37.93)	21 (36.21)	
≥ 65	19 (65.52)	18 (62.07)	37 (63.79)	
Fever				0.056

Continued Table 1. Patient demographic and clinical characteristics.

Parameter	Short disease course (n = 29)	Long disease course (n = 29)	All (N = 58)	P
No	14 (48.28)	7 (24.14)	21 (36.21)	
Yes	15 (51.72)	22 (75.86)	37 (63.79)	
Cough				0.401
No	11 (37.93)	8 (27.59)	19 (32.76)	
Yes	18 (62.07)	21 (72.41)	39 (67.24)	
Dyspnea				0.195
No	21 (72.41)	25 (86.21)	46 (79.31)	
Yes	8 (27.59)	4 (13.79)	12 (20.69)	
Rhinorrhea				1.000
No	29 (100.00)	28 (96.55)	57 (98.28)	
Yes	0	1 (3.45)	1 (1.72)	
Pharyngalgia				1.000
No	29 (100.00)	28 (96.55)	57 (98.28)	
Yes	0	1 (3.45)	1 (1.72)	
Diarrhea				1.000
No	25 (86.21)	25 (86.21)	50 (86.21)	
Yes	4 (13.79)	4 (13.79)	8 (13.79)	
Vomiting				1.000
No	27 (93.10)	28 (96.55)	55 (94.83)	
Yes	2 (6.90)	1 (3.45)	3 (5.17)	
Anorexia				0.164
No	26 (89.66)	22 (75.86)	48 (82.76)	
Yes	3 (10.34)	7 (24.14)	10 (17.24)	
Abdominal pain				1.000
No	29 (100.00)	28 (96.55)	57 (98.28)	
Yes	0	1 (3.45)	1 (1.72)	
Anosphrasia				1.000
No	29 (100.00)	28 (96.55)	57 (98.28)	
Yes	0	1 (3.45)	1 (1.72)	
Dysuria				1.000
No	28 (96.55)	29 (100.00)	57 (98.28)	
Yes	1 (3.45)	0	1 (1.72)	
Hypertension				1.000
No	14 (48.28)	14 (48.28)	28 (48.28)	
Yes	15 (51.72)	15 (51.72)	30 (51.72)	
Cardiovascular disease				1.000
No	26 (89.66)	27 (93.10)	53 (91.38)	
Yes	3 (10.34)	2 (6.90)	5 (8.62)	
Diabetes mellitus				0.517
No	22 (75.86)	24 (82.76)	46 (79.31)	
Yes	7 (24.14)	5 (17.24)	12 (20.69)	
Cerebrovascular disease				1.000
No	28 (96.55)	27 (93.10)	55 (94.83)	
Yes	1 (3.45)	2 (6.90)	3 (5.17)	
COPD				1.000
No	28 (96.55)	29 (100.00)	57 (98.28)	
Yes	1 (3.45)	0	1 (1.72)	
Chronic renal failure				1.000
No	29 (100.00)	28 (96.55)	57 (98.28)	
Yes	0	1 (3.45)	1 (1.72)	
Malignancy				1.000
No	28 (96.55)	28 (96.55)	56 (96.55)	
Yes	1 (3.45)	1 (3.45)	2 (3.45)	
Hepatitis				1.000
No	28 (96.55)	28 (96.55)	56 (96.55)	
Yes	1 (3.45)	1 (3.45)	2 (3.45)	
Smoking history				1.000
No	25 (86.21)	25 (86.21)	50 (86.21)	
Yes	4 (13.79)	4 (13.79)	8 (13.79)	

Data presented as mean±standard deviation, or count (percentage).

Short disease course = 9-18 days; Long disease course = 19-40 days.

ALT, alanine aminotransferase; AST, aspartate aminotransferase; BMI, body mass index; COPD, chronic obstructive pulmonary disease; CT, computed tomography; LDH, lactate dehydrogenase; hsCRP, high-sensitivity C-reactive protein; WBC, white blood cell.

Table 2. Demographic and clinical characteristics of patients with a short disease course by disease severity.

Parameter	Mild disease (n = 18)	Severe disease (n = 11)	p
Age	62.39±15.70	72.00±9.97	0.081
BMI, kg/m ²	24.49±1.62	23.41±4.70	0.470
Onset to CT, day	13.56±2.66	13.82±2.82	0.803
WBC count, ×10 ⁹	5.67±1.96	6.56±2.36	0.284
Lymphocytes, ×10 ⁹	1.29±0.43	0.94±0.35	0.035
Platelet count, ×10 ⁹	229.11±90.12	274.73±106.59	0.228
Hemoglobin, g/L	126.44±15.53	126.82±17.13	0.952
Prothrombin time, s	13.22±0.73	13.75±0.89	0.096
D-dimer, mg/L	0.81±0.79	3.75±3.56	0.002
hsCPR, mg/L	20.07±29.85	78.65±55.08	<0.001
ALT, U/L	42.56±45.95	29.91±19.95	0.397
AST, U/L	34.94±31.40	35.64±21.03	0.949
Albumin, g/L	38.11±4.25	33.82±4.01	0.012
Total bilirubin, μmol/L	9.89±6.41	13.57±6.67	0.151
Lactate dehydrogenase, U/L	278.67±135.70	339.45±173.46	0.302
Creatinine, μmol/L	72.72±17.21	91.27±46.35	0.134
Glucose, mmol/L	5.92±1.48	8.68±3.97	0.012
Procalcitonin, ng/L	0.10±0.09	0.19±0.21	0.127
Sex			0.316
Male	8 (44.44)	7 (63.64)	
Female	10 (55.56)	4 (36.36)	
Age, years			0.694
< 65	7 (38.89)	3 (27.27)	
≥ 65	11 (61.11)	8 (72.73)	
Fever			0.316
No	10 (55.56)	4 (36.36)	
Yes	8 (44.44)	7 (63.64)	
Cough			1.000
No	7 (38.89)	4 (36.36)	
Yes	11 (61.11)	7 (63.64)	
Dyspnea			0.433
No	14 (77.78)	7 (63.64)	
Yes	4 (22.22)	4 (36.36)	
Rhinorrhea			1.000
No	18 (100.00)	11 (100.00)	
Yes	0	0	
Pharyngalgia			1.000
No	18 (100.00)	11 (100.00)	
Yes	0	0	
Diarrhea			1.000
No	15 (83.33)	10 (90.91)	
Yes	3 (16.67)	1 (9.09)	
Vomiting			1.000
No	17 (94.44)	10 (90.91)	

Data presented as mean±standard deviation, or count (percentage).

Short disease course = 9-18 days; Long disease course = 19-40 days.

ALT, alanine aminotransferase; AST, aspartate aminotransferase; BMI, body mass index; COPD, chronic obstructive pulmonary disease; CT, computed tomography; LDH, lactate dehydrogenase; hsCPR, high-sensitivity C-reactive protein; WBC, white blood cell.

Continued Table 2. Demographic and clinical characteristics of patients with a short disease course by disease severity.

Parameter	Mild disease (n = 18)	Severe disease (n = 11)	p
Yes	1 (5.56)	1 (9.09)	
Anorexia			0.539
No	17 (94.44)	9 (81.82)	
Yes	1 (5.56)	2 (18.18)	
Abdominal pain			1.000
No	18 (100.00)	11 (100.00)	
Yes	0	0	
Anosmia			1.000
No	18 (100.00)	11 (100.00)	
Yes	0	0	
Dysuria			1.000
No	17 (94.44)	11 (100.00)	
Yes	1 (5.56)	0	
Hypertension			0.316
No	10 (55.56)	4 (36.36)	
Yes	8 (44.44)	7 (63.64)	
Cardiovascular disease			0.539
No	17 (94.44)	9 (81.82)	
Yes	1 (5.56)	2 (18.18)	
Diabetes mellitus			0.375
No	15 (83.33)	7 (63.64)	
Yes	3 (16.67)	4 (36.36)	
Cerebrovascular disease			1.000
No	17 (94.44)	11 (100.00)	
Yes	1 (5.56)	0	
COPD			1.000
No	17 (94.44)	11 (100.00)	
Yes	1 (5.56)	0	
Chronic renal failure			1.000
No	18 (100.00)	11 (100.00)	
Yes	0	0	
Malignancy tumor			1.000
No	17 (94.44)	11 (100.00)	
Yes	1 (5.56)	0	
Hepatitis			0.379
No	18 (100.00)	10 (90.91)	
Yes	0	1 (9.09)	
Smoking history			1.000
No	15 (83.33)	10 (90.91)	
Yes	3 (16.67)	1 (9.09)	

Table 3. Demographic and clinical characteristics of patients with a long disease course by disease severity.

Parameters	Mild disease (n = 17)	Severe disease (n = 12)	P
Age	65.29±11.69	67.17±11.48	0.672
BMI, kg/m ²	24.60±3.48	22.52±3.59	0.293
Onset to CT, day	24.65±5.22	24.83±7.59	0.938
WBC count, ×10 ⁹	6.17±4.18	8.40±4.69	0.190
Lymphocytes, ×10 ⁹	1.63±0.85	1.11±0.34	0.053
Platelet count, ×10 ⁹	297.94±84.94	279.83±102.24	0.607
Hemoglobin, g/L	121.12±18.51	120.58±17.86	0.939
Prothrombin time, s	13.73±1.01	14.23±1.44	0.299
D-dimer, mg/L	0.91±1.16	3.76±4.94	0.040
hsCPR, mg/L	6.28±9.34	16.65±14.01	0.024
ALT, U/L	18.59±11.65	39.08±36.25	0.037
AST, U/L	19.47±4.72	31.17±24.45	0.063
Albumin, g/L	39.01±2.61	32.18±3.65	<0.001
Total bilirubin, μmol/L	7.94±4.64	11.21±6.71	0.131
Lactate dehydrogenase, U/L	235.29±64.22	310.50±125.14	0.043
Creatinine, μmol/L	99.65±136.59	69.58±22.81	0.459
Glucose, mmol/L	6.65±3.24	6.81±2.43	0.885
Procalcitonin, ng/L	20.82±82.98	0.09±0.07	0.397
Sex			0.047
Male	5 (29.41)	8 (66.67)	
Female	12 (70.59)	4 (33.33)	
Age, years			0.668
< 65	7 (41.18)	4 (33.33)	
≥ 65	10 (58.82)	8 (66.67)	
Fever			0.665
No	5 (29.41)	2 (16.67)	
Yes	12 (70.59)	10 (83.33)	
Cough			0.683
No	4 (23.53)	4 (33.33)	
Yes	13 (76.47)	8 (66.67)	
Dyspnea			1.000
No	15 (88.24)	10 (83.33)	
Yes	2 (11.76)	2 (16.67)	
Rhinorrhea			1.000
No	16 (94.12)	12 (100.00)	
Yes	1 (5.88)	0	
Pharyngalgia			1.000
No	16 (94.12)	12 (100.00)	
Yes	1 (5.88)	0	
Diarrhea			0.622
No	14 (82.35)	11 (91.67)	
Yes	3 (17.65)	1 (8.33)	
Vomiting			0.414
No	17 (100.00)	11 (91.67)	

Data presented as mean±standard deviation, or count (percentage).

Short disease course = 9-18 days; Long disease course = 19-40 days.

ALT, alanine aminotransferase; AST, aspartate aminotransferase; BMI, body mass index; COPD, chronic obstructive pulmonary disease; CT, computed tomography; LDH, lactate dehydrogenase; hsCPR, high-sensitivity C-reactive protein; WBC, white blood cell.

Continued Table 3. Demographic and clinical characteristics of patients with a long disease course by disease severity.

Parameters	Mild disease (n = 17)	Severe disease (n = 12)	P
Yes	0	1 (8.33)	
Anorexia			1.000
No	13 (76.47)	9 (75.00)	
Yes	4 (23.53)	3 (25.00)	
Abdominal pain			0.414
No	17 (100.00)	11 (91.67)	
Yes	0	1 (8.33)	
Anosphrasia			1.000
No	16 (94.12)	12 (100.00)	
Yes	1 (5.88)	0	
Dysuria			1.000
No	17 (100.00)	12 (100.00)	
Yes	0	0	
Hypertension			0.710
No	9 (52.94)	5 (41.67)	
Yes	8 (47.06)	7 (58.33)	
Cardiovascular disease			1.000
No	16 (94.12)	11 (91.67)	
Yes	1 (5.88)	1 (8.33)	
Diabetes mellitus			1.000
No	14 (82.35)	10 (83.33)	
Yes	3 (17.65)	2 (16.67)	
Cerebrovascular disease			1.000
No	16 (94.12)	11 (91.67)	
Yes	1 (5.88)	1 (8.33)	
COPD			1.000
No	17 (100.00)	12 (100.00)	
Yes	0	0	
Chronic renal function failure			1.000
No	16 (94.12)	12 (100.00)	
Yes	1 (5.88)	0	
Malignancy tumor			0.414
No	17 (100.00)	11 (91.67)	
Yes	0	1 (8.33)	
Hepatitis			1.000
No	16 (94.12)	12 (100.00)	
Yes	1 (5.88)	0	
Smoking history			0.279
No	16 (94.12)	9 (75.00)	
Yes	1 (5.88)	3 (25.00)	

Table 4. Computed tomography findings in patients with a short disease course with mild or severe disease.

Parameter	Mild (n = 18)	Severe (n = 11)	P
Lower right lobe involvement			0.512
No	2 (11.11)	0	
Yes	16 (88.89)	11 (100.00)	
Right middle lobe involvement			0.058
No	6 (33.33)	0	
Yes	12 (66.67)	11 (100.00)	
Right upper lobe involvement			0.012
No	8 (44.44)	0	
Yes	10 (55.56)	11 (100.00)	
Left lower lobe involvement			0.268
No	3 (16.67)	0	
Yes	15 (83.33)	11 (100.00)	
Left upper lobe involvement			0.058
No	6 (33.33)	0	
Yes	12 (66.67)	11 (100.00)	
Number of affected lobes			0.013
1	2 (11.11)	0	
2	3 (16.67)	0	
3	3 (16.67)	0	
4	2 (11.11)	0	
5	8 (44.44)	11 (100.00)	
Lung involvement			0.268
Unilateral	3 (16.67)	0	
Bilateral	15 (83.33)	11 (100.00)	
Mediastinal lymphadenopathy			0.339
No	16 (88.89)	8 (72.73)	
Yes	2 (11.11)	3 (27.27)	
Hilar lymphadenopathy			1.000
No	18 (100.00)	11 (100.00)	
Yes	0	0	
Axillary lymphadenopathy			1.000
No	18 (100.00)	11 (100.00)	
Yes	0	0	
Pericardial effusion			0.018
No	17 (94.44)	6 (54.55)	
Yes	1 (5.56)	5 (45.45)	
Pleural effusion			0.050
None	16 (88.89)	6 (54.55)	
Unilateral	2 (11.11)	3 (27.27)	
Bilateral	0	2 (18.18)	
Pleural thickening			<0.001
None	7 (38.89)	0	
Unilateral	5 (27.78)	0	
Bilateral	6 (33.33)	11 (100.00)	
Pleural involvement			0.026

Data presented as count (percentage).

Short disease course = 9-18 days; Long disease course = 19-40 days.

ICU, intensive care unit.

Continued Table 4. Computed tomography findings in patients with a short disease course with mild or severe disease.

Parameter	Mild (n = 18)	Severe (n = 11)	P
No	7 (38.89)	0	
Yes	11 (61.11)	11 (100.00)	
Subpleural lesion			1.000
No	0	0	
Yes	18 (100.00)	11 (100.00)	
Grid shadow			0.012
No	8 (44.44)	0	
Yes	10 (55.56)	11 (100.00)	
Higher-density vascular shadows			0.026
No	7 (38.89)	0	
Yes	11 (61.11)	11 (100.00)	
Crazy-paving appearance			0.003
No	10 (55.56)	0	
Yes	8 (44.44)	11 (100.00)	
Nodules			0.438
No	6 (33.33)	6 (54.55)	
Yes	12 (66.67)	5 (45.45)	
Lung consolidation			0.026
No	7 (38.89)	0	
Yes	11 (61.11)	11 (100.00)	
Air bronchogram sign			0.006
No	12 (66.67)	1 (9.09)	
Yes	6 (33.33)	10 (90.91)	
Ground-glass opacities			0.694
No	11 (61.11)	8 (72.73)	
Yes	7 (38.89)	3 (27.27)	
Nodular halo sign			0.512
No	16 (88.89)	11 (100.00)	
Yes	2 (11.11)	0	
Fibrous foci			0.026
No	7 (38.89)	0	
Yes	11 (61.11)	11 (100.00)	
Atelectasis			0.114
No	14 (77.78)	5 (45.45)	
Yes	4 (22.22)	6 (54.55)	
Mosaic sign			1.000
No	17 (94.44)	10 (90.91)	
Yes	1 (5.56)	1 (9.09)	
Pleural effusion			0.071
No	16 (88.89)	6 (54.55)	
Yes	2 (11.11)	5 (45.45)	
Outcome			0.199
Discharged	4 (22.22)	1 (9.09)	
Transferred to ICU	0	1 (9.09)	
No obvious change	0	1 (9.09)	
Symptom improvement	14 (77.78)	8 (72.73)	

Table 5. Computed tomography findings in patients with a long disease course with mild or severe disease.

Parameter	Mild disease (n = 17)	Severe disease (n = 12)	P
Lower right lobe involvement			1.000
No	1 (5.88)	0	
Yes	16 (94.12)	12 (100.00)	
Right middle lobe involvement			0.023
No	7 (41.18)	0	
Yes	10 (58.82)	12 (100.00)	
Right upper lobe involvement			0.003
No	9 (52.94)	0	
Yes	8 (47.06)	12 (100.00)	
Left lower lobe involvement			0.121
No	4 (23.53)	0	
Yes	13 (76.47)	12 (100.00)	
Left upper lobe involvement			0.093
No	7 (41.18)	1 (8.33)	
Yes	10 (58.82)	11 (91.67)	
Number of affected lobes			0.009
1	3 (17.65)	0	
2	4 (23.53)	0	
3	2 (11.76)	0	
4	0	1 (8.33)	
5	8 (47.06)	11 (91.67)	
Lung involvement			0.059
Unilateral	5 (29.41)	0	
Bilateral	12 (70.59)	12 (100.00)	
Mediastinal lymphadenopathy			0.056
No	16 (94.12)	7 (58.33)	
Yes	1 (5.88)	5 (41.67)	
Hilar lymphadenopathy			1.000
No	17 (100.00)	12 (100.00)	
Yes	0	0	
Axillary lymphadenopathy			0.414
No	17 (100.00)	11 (91.67)	
Yes	0	1 (8.33)	
Pericardial effusion			0.403
No	14 (82.35)	8 (66.67)	
Yes	3 (17.65)	4 (33.33)	
Pleural effusion			0.001
0	15 (88.24)	3 (25.00)	
1	2 (11.76)	6 (50.00)	
2	0	3 (25.00)	
Pleural thickening			0.007
0	5 (29.41)	0	
1	5 (29.41)	1 (8.33)	
2	7 (41.18)	11 (91.67)	

Data presented as count (percentage).

Short disease course = 9-18 days; Long disease course = 19-40 days.

ICU, intensive care unit.

Continued Table 5. Computed tomography findings in patients with a long disease course with mild or severe disease.

Parameter	Mild disease (n = 17)	Severe disease (n = 12)	P
Subpleural lesion			1.000
No	0	0	
Yes	17 (100.00)	12 (100.00)	
Grid shadow			<0.001
No	13 (76.47)	0	
Yes	4 (23.53)	12 (100.00)	
Higher-density vascular shadows			0.001
No	10 (58.82)	0	
Yes	7 (41.18)	12 (100.00)	
Crazy-paving appearance			<0.001
No	13 (76.47)	0	
Yes	4 (23.53)	12 (100.00)	
Nodules			0.703
No	9 (52.94)	8 (66.67)	
Yes	8 (47.06)	4 (33.33)	
Lung consolidation			0.001
No	10 (58.82)	0	
Yes	7 (41.18)	12 (100.00)	
Air bronchogram sign			<0.001
No	15 (88.24)	1 (8.33)	
Yes	2 (11.76)	11 (91.67)	
Ground-glass opacities			0.403
No	14 (82.35)	8 (66.67)	
Yes	3 (17.65)	4 (33.33)	
Nodular halo sign			0.498
No	15 (88.24)	12 (100.00)	
Yes	2 (11.76)	0	
Fibrous foci			0.408
No	6 (35.29)	2 (16.67)	
Yes	11 (64.71)	10 (83.33)	
Atelectasis			0.014
No	15 (88.24)	5 (41.67)	
Yes	2 (11.76)	7 (58.33)	
Mosaic sign			1.000
No	17 (100.00)	12 (100.00)	
Yes	0	0	
Pleural effusion			0.001
No	15 (88.24)	3 (25.00)	
Yes	2 (11.76)	9 (75.00)	
Outcome			0.024
Discharged	6 (35.29)	0	
Transferred to ICU	0	0	
No obvious change	1 (5.88)	1 (8.33)	
Symptom improvement	10 (58.82)	11 (91.67)	

Table 6. Summary of computed tomography (CT) features significantly correlated with greater disease severity in patients with a short disease course and those with a long disease course.

CT features correlated with greater disease severity in patients with a short disease course	CT features correlated with greater disease severity in patients with a long disease course
Right middle lobe	Right middle lobe
Right upper lobe	Right upper lobe
Left upper lobe	Left upper lobe
Number of affected lobes	Number of affected lobes
	Bilateral lung involvement
	Mediastinal lymphadenopathy
Pericardial effusion	
Pleural effusion	Pleural effusion
Pleural thickening	Pleural thickening
Pleural involvement	Pleural involvement
Grid shadow	Grid shadow
Higher-density vascular shadows	Higher-density vascular shadows
Crazy-paving appearance	Crazy-paving appearance
Lung consolidation	Lung consolidation
Air bronchogram sign	Air bronchogram sign
Fibrous foci	
	Atelectasis

All correlations were significant at a 2-tailed value of $P < 0.05$.
Short disease course = 9-18 days; Long disease course = 19-40 days.

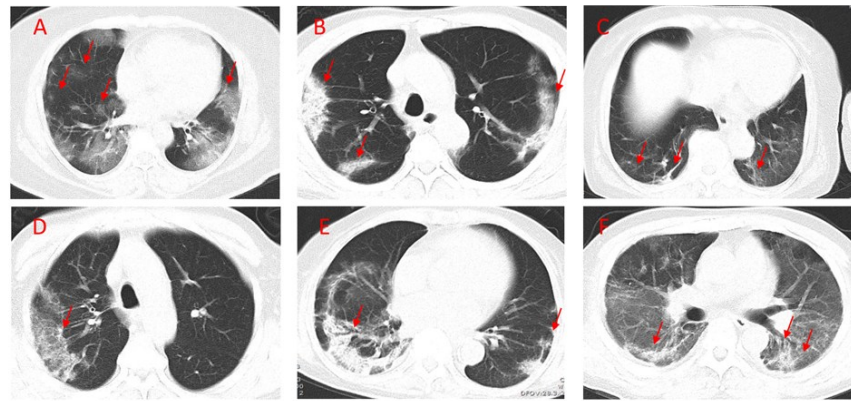


Figure 1. Representative chest CT images in several COVID-19 patients. (A) 58-year-old female, day 14 after symptom onset: bilateral multi-focal ground-glass and nodules in the right upper lobe; (B) 81-year-old man, day 12 after symptom onset: bilateral predominant consolidation pattern, mainly located in the subpleural area, parallel to the pleura like a ribbon; (C) 78-year-old woman, day 13 after symptom onset: ground-glass opacities in bilateral lower lobe with fibrous lesions in the right lower lobe; (D) 78-year-old man, day 19 after symptom onset: ground-glass opacity, crazy-paving pattern and in the right lobe, mainly located below the pleura; (E) 82-year-old woman, day 20 after symptom onset: bilateral and subpleural predominant consolidation pattern, runs along the pleura in a parallel shape with air bronchograms in the right lobe; (F) 47-year-old man, day 34 after symptom onset: bilateral white lung with ground-glass opacities.

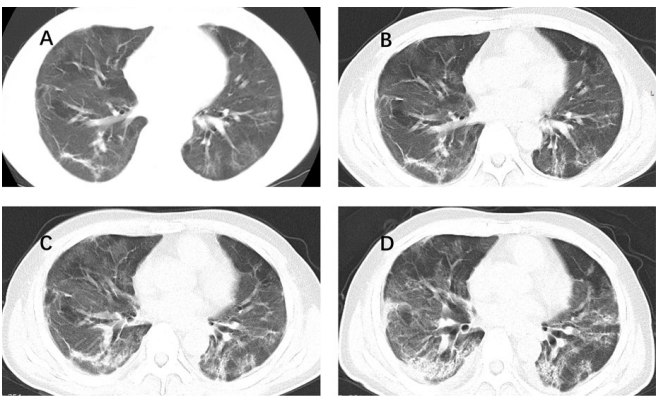


Figure 2. Chest CT images from a 47-year male. (A) Day 34 after symptom onset: Bilateral diffuse ground-glass opacities and consolidations, with air bronchograms inside (red arrow) with local thickening and adhesions of bilateral pleura; (B) Day 46: the lesions had decreased in extent and the density; (C) Day 53: the lesions continued to decrease in extent and the density; (D) Day 61: the lesions continued to decrease in extent and the density. The patient was ready for discharge from hospital after the final scan.

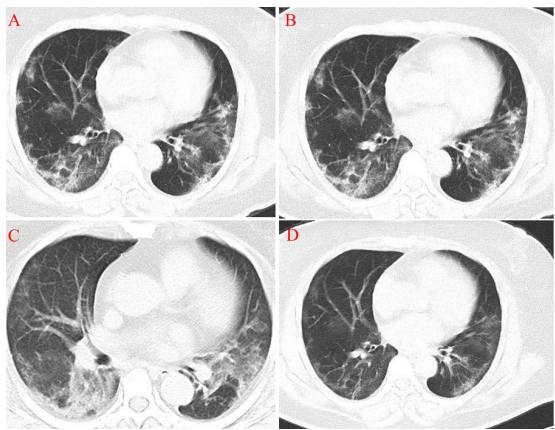


Figure 3. Chest CT images from a 58-year female. (A) Day 9 after symptom onset: Bilateral multifocal ground-glass opacities and partial consolidations, with local thickening and adhesions of bilateral pleura; (B) Day 17: the lesions had increased in extent and the density, with bilateral pleura thickening; (C) Day 23: the lesions increased in extent and the density and became heterogeneous, with air bronchograms inside (red arrow); (D) Day 30: the lesions continued to decrease in extent and the density. The patient was ready for discharge from hospital after the final scan.

DISCUSSION

In this study, we sought to determine differences in laboratory and CT findings between COVID-19 patients with a short vs. long disease course, and subgroups with mild vs. severe disease. Our results showed that while there were limited or no differences in laboratory results and CT findings between patients with a short vs. long disease course, but many significant differences could be found between mild and severe disease patients.

A great deal of research has been devoted to determining correlations and the predictive value of clinical, laboratory, and chest CT findings for COVID-19 severity and outcomes. Fan *et al.* ⁽¹⁴⁾ analyzed 86 COVID-19 patients and found that compared to the mild/moderate group, the severe/critical group had a significantly higher male ratio. Another two meta-analyses by Jutzeler *et al.* ⁽¹⁵⁾ and Borges do Nascimento *et al.* ⁽¹⁶⁾ also revealed that male COVID-19 patients were associated with severe disease. Furthermore, a Denmark nationwide study including 4,842 Covid-19 patients demonstrated that male patients had higher risks of severe Covid-19 diagnosis even after age and comorbidities were adjusted as confounding variables ⁽¹⁷⁾. Consistent with these findings, among patients with a long disease course in this study, the male ratio was significantly higher in severe disease patients than in mild disease patients. One of possible mechanisms underlying the differential risk in disease severity is that sex differences in the immunological response to Covid-19 infection, which could be attributed to X chromosomes ⁽¹⁸⁾. After viral infection, females produce higher levels of antibodies and less inflammatory cytokine interleukin-6 as compared with male patients ⁽¹⁸⁾. As a result, female patients are less susceptible to severe viral infections than male patients. Other proposed explanations include sex-related lifestyle differences (such as smoking, alcohol, and obesity) and comorbidities, which are all risk factors of severe Covid-19 ⁽¹⁹⁾. However, the underlying mechanism should be further elucidated.

Regarding laboratory results, a meta-analysis including 3396 COVID-19 patients by Ghahramani *et al.* ⁽²⁰⁾ has shown that the severe group had significant decreases in lymphocytes and albumin, and significant increases in ALT, CRP, and D-dimer as compared with the non-severe group. Another meta-analysis ⁽¹⁵⁾ reported that COVID-19 patients with severe disease had decreased albumin and increased levels of CRP as compared with the non-severe group. Borges do Nascimento *et al.* ⁽¹⁶⁾ meta-analysis also showed that elevated CRP levels were associated with severe disease. A meta-analysis showed that levels of D-dimer are significantly higher in severe COVID-19 patients than in mild disease patients ⁽²¹⁾. In line with these observations, the current study found that among both patients with

short and long disease courses, patients with severe disease had significantly higher hsCRP and D-dimer levels but lower albumin levels. In addition, compared to the mild disease patients, lymphocyte count was markedly reduced in severe disease patients among the short disease course group ($p=0.035$) and the long disease course group ($p=0.053$, margin significance). Meanwhile, the severe disease group had significantly elevated ALT levels than the mild disease group among the long disease course group.

CRP is a major positive acute-phase protein secreted by hepatocytes in response to interleukin-6 ^(22, 23) and is widely accepted as an inflammatory biomarker ⁽²⁴⁾. Therefore, the elevated CRP levels in severe COVID-19 patients may be attributed to the overproduction of inflammatory cytokines ⁽²⁵⁾. It has been reported that CRP levels were elevated significantly in COVID-19 patients with low oxygen saturation levels as compared with those with high oxygen saturation levels ⁽²⁶⁾, indicating that CRP levels well correlate with the severity of COVID-19 disease. D-dimer is a circulating peptide derived from fibrin degradation ⁽²⁷⁾ and is also an acute-phase protein ⁽²³⁾. Yao *et al.* also reported that D-dimer levels were well correlated with disease severity of COVID-19 and could be a biomarker predicting mortality ⁽²⁸⁾.

There are many reports of CT findings in COVID-19 patients. A meta-analysis including 60 studies and 5041 COVID-19 patients on CT imaging findings has demonstrated that pulmonary consolidation was mainly found in the severe and progressive stages of the disease, which can be accompanied by fibrotic lesions and GGO ⁽²⁹⁾. The authors suggested that these pathological changes could be attributed to interstitial thickening, inflammatory cell infiltration, hyaline membrane formation, and cell exudation. Consistent with their observation, the current study showed that lung consolidation was the CT feature that significantly correlated with greater disease severity in patients with both short and long disease courses. Moreover, fibrous foci were also a CT feature associated with greater disease severity in the short disease course group.

Kaya and Akman have reported that mediastinal lymphadenopathy is an important CT finding for predicting a severe prognosis in COVID-19 patients ⁽³⁰⁾. In line with this observation, our correlation analysis showed that among the long disease course group, mediastinal lymphadenopathy was associated with greater disease severity. Lan *et al.* have found that consolidation and subpleural atelectasis were more common in severe COVID-19 patients ⁽³¹⁾, which is also in agreement with our observation that atelectasis was a CT feature associated with greater disease severity in the long disease course group.

Ghantous *et al.* have investigated pericardial involvement in hospitalized patients with COVID-19

and found that patients with pericardial effusion had more severe disease⁽³²⁾. Our study also found that pericardial effusion was a CT feature correlated with greater disease severity in the short disease course group. A multi-center study including 102 mild COVID-19 cases and 50 severe cases revealed that⁽³³⁾ the severe group had significantly more bilateral lung involvement, lung consolidation, air bronchogram sign, crazy-paving sign, and the number of segments affected than the mild group⁽³³⁾. Interestingly, this study also found that bilateral lung involvement (only in patients with long disease course), lung consolidation, crazy-paving appearance, and more affected lobes were the CT features correlated with greater disease severity in patients with both short and long disease courses. All these findings indicated that CT features may potentially be used to predict disease severity in COVID-19. However, more studies are needed to validate their predictive performance.

In summary, this study showed that For COVID-19 patients with a short disease course pericardial effusion and fibrous foci were the CT findings correlated with greater disease severity. For those with a long disease course, bilateral lung involvement, mediastinal lymphadenopathy, and atelectasis were associated with greater disease severity. These findings may assist in identifying patients who may develop more severe diseases and require more intensive treatment.

Ethical consideration: This study was approved by the institutional review board of the Third Affiliated Hospital, Sun Yat-sen University (No. [2020] 02-159-01), and because of the retrospective nature of the study the requirement of patient informed consent was waived.

Author contributions: Yuqi Zhou and Wenjuan Li conceived and designed the study. Wenjuan Li acquired and analyzed the clinical data. Wenjuan Li and Yuqi Zhou conducted the statistical analysis. All authors wrote and reviewed the manuscript, and all authors approved the final version of the manuscript.

REFERENCES

- Huang C, Wang Y, Li X, et al. (2020) Clinical features of patients infected with 2019 novel coronavirus in Wuhan, China. *Lancet*, **395**(10223): 497–506.
- Lu R, Zhao X, Li J, et al. (2020) Genomic characterisation and epidemiology of 2019 novel coronavirus: implications for virus origins and receptor binding. *Lancet*, **395**(10224): 565–574.
- Ai T, Yang Z, Hou H, et al. (2020) Correlation of chest CT and RT-PCR testing for coronavirus disease 2019 (COVID-19) in China: A Report of 1014 Cases. *Radiology*, **296**(2): E32–E40.
- Cozzi D, Albanesi M, Cavigli E, et al. (2020) Chest X-ray in new Coronavirus Disease 2019 (COVID-19) infection: findings and correlation with clinical outcome. *Radiol Medica*, **125**(8): 730–737.
- Chung M, Bernheim A, Mei X, et al. (2020) CT imaging features of 2019 novel coronavirus (2019-nCoV). *Radiology*, **295**(1): 202–207.
- Hani C, Trieu NH, Saab I, Dangeard S, et al. (2020) COVID-19 pneumonia: A review of typical CT findings and differential diagnosis. *Diagn Interv Imaging*, **101**(5): 263–268.
- Ye Z, Zhang Y, Wang Y, et al. (2020) Chest CT manifestations of new coronavirus disease 2019 (COVID-19): a pictorial review. *Eur Radiol*, **30**(8): 4381–4389.
- de Farias L de PG, Fonseca EKUN, et al. (2020) Imaging findings in COVID-19 pneumonia. *Clinics*, **75**: e2027.
- Li B, Li X, Wang Y, Han Y, et al. (2020) Diagnostic value and key features of computed tomography in Coronavirus Disease 2019. *Emerg Microbes Infect*, **9**(1): 787–793.
- Wasilewski PG, Mruk B, Mazur S, et al. (2020) COVID-19 severity scoring systems in radiological imaging – A review. *Polish J Radiol*, **85**: e361–e368.
- Li M, Lei P, Zeng B, et al. (2020) Coronavirus Disease (COVID-19): Spectrum of CT Findings and Temporal Progression of the Disease. *Acad Radiol*, **27**(5): 603–608.
- Sun Z, Zhang N, Li Y, Xu X (2020) A systematic review of chest imaging findings in COVID-19. *Quant Imaging Med Surg*, **10**(5): 1058–1079.
- Tabatabaei SMH, Rahimi H, Moghaddas F, Rajebi H (2020) Predictive value of CT in the short-term mortality of Coronavirus Disease 2019 (COVID-19) pneumonia in nonelderly patients: A case-control study. *Eur J Radiol*, **132**: 109298.
- Fan L, Le W, Zou Q, et al. (2021) Initial CT features of COVID-19 predicting clinical category. *Chin J Acad Radiol*, **4**(4): 241–247.
- Jutzeler CR, Bourguignon L, Weis CV, et al. (2020) Comorbidities, clinical signs and symptoms, laboratory findings, imaging features, treatment strategies, and outcomes in adult and pediatric patients with COVID-19: A systematic review and meta-analysis. *Travel Med Infect Dis*, **37**: 101825.
- do Nascimento IJB, von Groote TC, O'Mathúna DP, et al. (2020) Clinical, laboratory and radiological characteristics and outcomes of novel coronavirus (SARS-CoV-2) infection in humans: A systematic review and series of meta-analyses. *PLoS One*, **15**(9): e0239235.
- Kragholm K, Andersen MP, Gerds TA, et al. (2021) Association Between Male Sex and Outcomes of Coronavirus Disease 2019 (COVID-19)-A Danish Nationwide, Register-based Study. *Clin Infect Dis*, **73**(11): E4025–E4030.
- Conti P and Younes A (2020) Coronavirus cov-19/sars-cov-2 affects women less than men: Clinical response to viral infection. *J Biol Regul Homeost Agents*, **34**(2): 339–343.
- Cai H (2020) Sex difference and smoking predisposition in patients with COVID-19. *Lancet Respir Med*, **8**(4): e20.
- Ghahramani S, Tabrizi R, Lankarani KB, et al. (2020) Laboratory features of severe vs. non-severe COVID-19 patients in Asian populations: A systematic review and meta-analysis. *Eur J Med Res*, **25**(1): 30.
- Paliogiannis P, Mangoni AA, Dettori P, et al. (2020) D-dimer concentrations and covid-19 severity: A systematic review and meta-analysis. *Front Public Heal*, **8**: 1–7.
- Morley JJ and Kushner I (1982) Serum C-reactive protein levels in disease. *Ann N Y Acad Sci*, **389**: 406–418.
- Jain S, Gautam V, Naseem S (2011) Acute-phase proteins: As diagnostic tool. *J Pharm Bioallied Sci*, **3**: 118–127.
- Luan YY and Yao YM (2018) The Clinical Significance and Potential Role of C-Reactive Protein in Chronic Inflammatory and Neurodegenerative Diseases. *Front Immunol*, **9**: 1302.
- Ali N (2020) Elevated level of C-reactive protein may be an early marker to predict risk for severity of COVID-19. *J Med Virol*, **92**(11): 2409.
- Xie J, Covassin N, Fan Z, et al. (2020) Association Between Hypoxemia and Mortality in Patients With COVID-19. *Mayo Clin Proc*, **95**(6): 1138–1147.
- Moresco RN, Vargas LCR, Voegeli CF, Vianna Santos RC (2003) D-dimer and its relationship to fibrinogen/fibrin degradation products (FDPs) in disorders associated with activation of coagulation or fibrinolytic systems. *J Clin Lab Anal*, **17**(3): 77.
- Yao Y, Cao J, Wang Q, et al. (2020) D-dimer as a biomarker for disease severity and mortality in COVID-19 patients: A case control study. *J Intensive Care*, **8**: 1–11.
- Awulachew E, Diriba K, Anja A, Getu E, Belayneh F (2020) Computed Tomography (CT) Imaging Features of Patients with COVID-19: Systematic Review and Meta-Analysis. *Radiol Res Pract*, **2020**: 1023506.
- Kaya AT and Akman B (2022) Mediastinal lymph node enlargement in COVID-19: Relationships with mortality and CT findings. *Hear Lung*, **54**: 19.
- Lan GY, Lee YJ, Wu JC, et al. (2022) Serial quantitative chest computed tomography imaging as prognosticators of coronavirus disease 2019 pneumonia. *J Formos Med Assoc*, **121**(3): 718–722.
- Ghantous E, Szekely Y, Lichter Y, et al. (2022) Pericardial Involvement in patients hospitalized with COVID-19: prevalence, associates, and clinical implications. *J Am Heart Assoc*, **11**(7): 24363.
- Yu Y, Wang X, Li M, et al. (2020) Nomogram to identify severe coronavirus disease 2019 (COVID-19) based on initial clinical and CT characteristics: a multi-center study. *BMC Med Imaging*, **20**(1): 111.

